Hydrocarbon Sensing Mechanism of Surface Ruthenated Tin Oxide: An In Situ IR, ESR, and Adsorption Kinetics Study

V. A. Chaudhary, I. S. Mulla, and K. Vijayamohanan*

Physical and Materials Chemistry Division

S. G. Hegde and D. Srinivas

Catalysis Division, National Chemical Laboratory, Pune 411008, India

Received: August 2, 2000; In Final Form: November 13, 2000

In this study we explain the conductivity changes involved in the sensing mechanism of surface ruthenated tin oxide toward butane. The adsorption free energy is found to be higher for surface ruthenated tin oxide ($\Delta G = -64.85$ kJ/mol) as compared to pure tin oxide ($\Delta G = -50.2$ kJ/mol) implying that the gas adsorbs faster on the ruthenated sample. The ESR studies indicate that butane preferentially adsorbs on the Ru sites, while the IR studies explain the nature of the adsorbed species. A scheme based on these studies is proposed, where surface acetate species is formed on the surface ruthenated tin oxide upon adsorption of butane at 300 °C, while the electronic conduction in these sensors is attributed to the formation of surface states.

Introduction

The surface electronic structure of metal oxides play an important role in their use in many technological applications such as catalysis,[1−3] chemical sensing,[4−6] and high efficiency solar cells.[7] The bulk electronic properties of tin oxide have been widely studied,[8,9] but the surface electronic properties are little understood especially since the electronic properties of the surface can vary drastically from the bulk. Tin oxide is a wide band gap semiconducting oxide ($E_g = 3.6$ eV) crystallizing in the rutile structure (six atoms per tetragonal unit cell). The energy band structure of this oxide has been calculated several times using a LCAO calculation of s and p orbitals.[10,11] The valence band is mainly composed of O_{2p} orbitals and the conduction band consists of Sn_{5s} and Sn_{5p} orbitals. Regarding the surface electronic structure, a significant amount of photo-emission work is available, about (110) and (001) surfaces which indicate an oxygen deficit surface displaying a significant density of surface states in the band gap up to the Fermi level. Completely oxidized surfaces do not show this. Recent studies have established that the formation of surface states in the mid gap region is one of the factors that is responsible for the gas sensing behavior of tin oxide. In particular, artificial creation of surface states in the band gap of tin oxide by using different noble metals, such as Pd, Ag, Pt, etc., can lead to a drastic change in the electrical properties of tin oxide. These surface states can also effectively induce the adsorption of gases onto the surface of tin oxide at higher temperatures thus altering the electronic properties significantly. Hence a deliberate modification of the surface can be effectively used in controlling the gas sensing behavior.

Our previous studies have shown that the surface functionalization of tin oxide using covalent anchoring of ruthenium and other species, such as Pd, Pt, and Ag, from solution can be very effective in getting selectivity control.[12,13] A systematic evaluation of the coverage, sensitivity, selectivity, morphology,
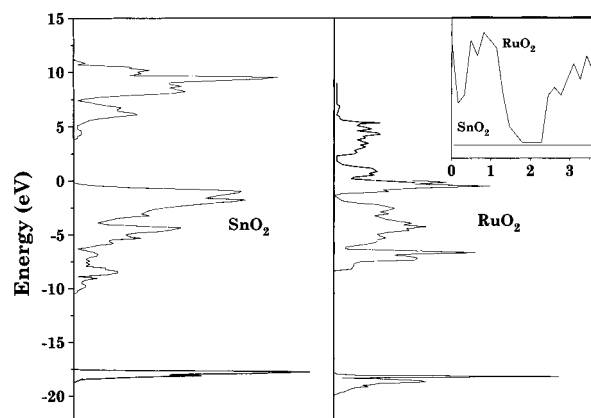
oxidation state, and thermal stability indicates that the amount and distribution of the grafted RuO_2 is the most important parameter in controlling the electrical transport with hydrocarbon adsorption. RuO_2 also has a rutile structure and helps in introducing band gap states in tin oxide. A comparison of the theoretical valence band DOS of SnO_2 and RuO_2[10,14] indicates that the Ru_{4d} and Ru_{5s} orbitals can lead to the creation of surface states in the mid gap region of tin oxide (Figure 1). These adsorbed Ru cations help to maintain SnO environments due to the generation of defect states near the valence band maximum. The visible effect of this is the enhancement in sensitivity of the ruthenated tin oxide in comparison to pure tin oxide to 1000 ppm of LPG at 300 °C.[15] All gas adsorption phenomena on semiconductors, in principle should involve the formation of surface states (at least in the initial time domain) and the submonolayer coverage valid for sensors (ppm and ppb range of the analyte) is particularly significant since there are no sufficient molecules for two-dimensional condensation. Impedance measurements of bare and surface ruthenated tin oxide vis-à-vis hydrocarbon adsorption indicates the importance of surface states in the sensing mechanism.[16]

Though we have established the importance of surface states in gas sensing, the exact mechanism of gas sensing is still not very clear. In the present report we attempt to give a plausible mechanism for gas sensing of surface ruthenated tin oxide. More specifically a systematic study of this system using various in situ techniques such as IR (infrared spectroscopy) and ESR (electron spin resonance spectroscopy) indicates the role of Ru cations and the species which are formed on the surface of the ruthenated tin oxide.

Experimental Section

The preparation of the samples has already been described in our previous reports.[12,13] In brief, tin oxide powder either obtained commercially or prepared by the precipitation method, was mixed thoroughly with binder using acetone and pressed into pellets. These pellets were sintered at 650 °C and then

* To whom correspondence should be addressesd. E-mail: viji@ ems.ncl.res.in. Fax: 0091-020-5983044.

Figure 1. Density of states in SnO_2 and RuO_2 (inset indicates the region between 0 and 3.6 eV).

Figure 2. ESR spectra of pure tin oxide (a) before and (b) after exposure to butane gas.

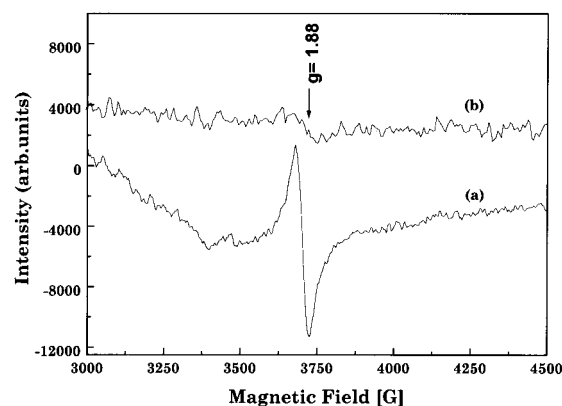**Figure 3.** ESR spectra of ruthenated tin oxide (a) before and (b) after exposure to gas.

surface modifed with Ru species via solution route. For all the studies, the optimum samples (0.27 wt % Ru on the surface having highest sensitivity toward 1000 ppm of hydrocarbons at 300 °C) were used for each measurement.

For both ESR and IR measurements tin oxide powder modified with 0.27 wt % RuO_2 was used. ESR investigations were carried out on a Bruker EMX X-band ($\nu = 9.75$ GHz) spectrometer using a 100 kHz field modulation. The measurement frequency was monitored by using a microwave frequency counter built in the Bruker ER 041× D−G microwave bridge. An organic free radical Diphenyl-picrylhydrazine (DPPH) was used as a field marker ($g = 2.0036$). Experiments were performed at room temperature in Suprasil quartz tubes (3.5 mm diameter) and the spectra were recorded by averaging over 15 cycles. ESR spectra were recorded for both pure and surface ruthenated tin oxide powders before and after exposing to butane. The sample was preheated at 300 °C in air for 2 h and then exposed to butane gas (20 mm pressure) for 2 h. The samples were then cooled in the presence of butane gas at the rate of 1 °C/min to room temperature. The gas was then flushed by using argon and subjected to ESR studies.

The FTIR spectra were recorded on a NICOLET 60 SXB spectrometer in transmission mode using self-supported wafers. Pure and surface ruthenated tin oxide powders were pressed into thin wafers weighing about $10-12$ mg/cm^2 by applying a pressure of 7 tons/in.^{2} The wafers were then mounted on the sample holder and placed in the sample compartment of the FTIR spectrometer. The sample was heated slowly (200 °C/h) "in situ" under vacuum (10^{-5} Torr) to 300 °C and held at that temperature for 2 h. Then, pure oxygen (75 mm Torr pressure) was introduced and the temperature was maintained for another 2 h. This conditioning was carried out for all the samples. This was followed by cooling the sample to 200 °C and introducing ultrapure *n*-butane gas at a partial pressure of 20 mm. The IR spectra were recorded at regular time intervals in order to study the formation of the reacted species with time upon adsorption of butane gas. A similar treatment was carried out for the samples at 300 and 50 °C. For comparison IR spectra of the pure and ruthenated sample were also recorded after evacuation of the cell (after exposure to butane gas) at different temperatures. All the spectra were scanned with 4 cm^{-1} resolution, averaging over 500 scans.

Results and Discussion

Figure 2 shows the ESR spectra of pure tin oxide with and without exposure to butane gas. Pure SnO_2 shows a broad hump and a signal corresponding to a *g* value of 1.88. This is probably
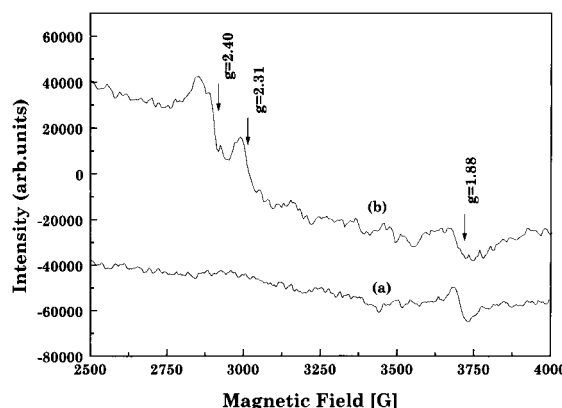
due to the Fe impurities present in tin oxide. In contrast to the previous report[17] there is no indication of the O_2^- species. This may be because the sample is stoichiometric with very few defects and less porous enabling a minimal amount of oxygen to be adsorbed onto the surface. On exposure to butane, the intensity of the signal corresponding to $g = 1.88$ decreases. This implies that the Fe species changes its oxidation state upon adsorption. However, the sensitivity measurements of pure and ruthenated tin oxide[15] clearly indicates that the Fe sites are not responsible for the enhanced sensitivity of surface ruthenated tin oxide. The amount of Fe in tin oxide is negligible and though the ESR studies indicate that the state of Fe changes on adsorption of gas it may not play a major role in gas sensing.

The ESR spectra of surface ruthenated sample before and after exposure to gas are shown in Figure 3. The ESR spectrum of the ruthenated sample before exposure to gas gives a signal ($g = 1.88$) corresponding only to the Fe species in tin oxide. There is no signal corresponding to the Ru species implying that Ru is present in Ru^{4+} state which is also confirmed by XPS studies. However, the sample after adsorption of gas shows interesting changes. Additional signals appear corresponding to a *g*-factor of 2.40 and 2.31 respectively, which is attributed to Ru^{3+} species. This implies that the Ru^{4+} species is converted to Ru^{3+} species due to the adsorption of gas. The gas may preferentially adsorb on the Ru sites donating an electron in the process. Thus, the Ru sites act as a catalyst for increased adsorption of the gas molecules which is also confirmed by the increased sensitivity of the ruthenated samples in comparison to that of the pure tin oxide samples.[15] The visible effect of this is also indicated by comparing the adsorption kinetics of the gas on the pure and ruthenated samples as discussed below.

Surface Ruthenated Tin Oxide

J. Phys. Chem. B, Vol. 105, No. 13, 2001 **2567**
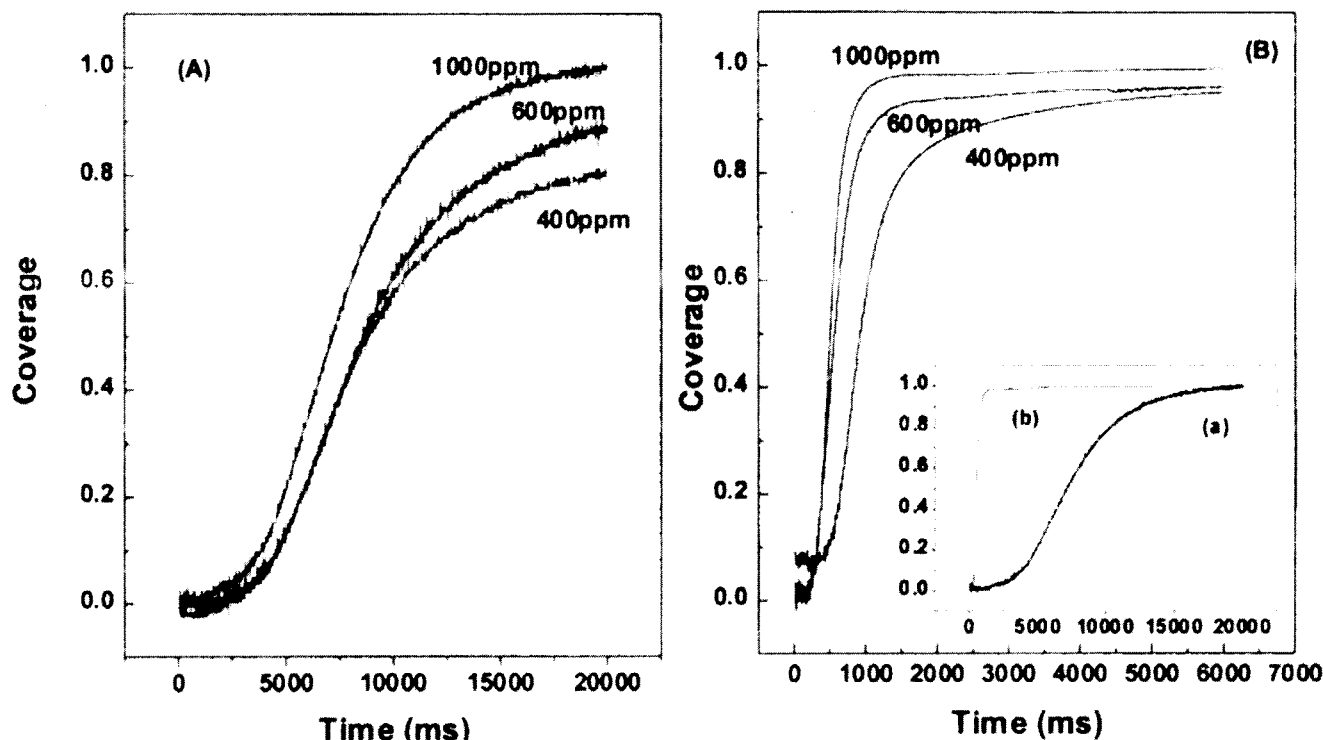
Figure 4. Variation of gas coverage with time for (A) pure and (B) surface ruthenated tin oxide at different concentrations of LPG at 300 °C. (Inset: Comparison of the adsorption kinetics of 1000 ppm butane on (a) pure and (b) surface ruthenated samples at 300 °C).

To understand the adsorption kinetics of butane at 300 °C on surface ruthenated tin oxide, coverage vs time plots were derived from the observed resistance variation with time.[15] Figure 4 shows these plots for (A) the pure and (B) ruthenated samples at different concentrations of butane at 300 °C. For pure tin oxide the attainment of equilibrium coverage is very slow in comparison with similar change for the surface ruthenated sample although, in both cases the saturation coverage is reached asymptotically. This process of attainment of equilibrium coverage becomes increasingly sluggish for both the cases with decrease in gas concentration. The steep coverage variation both at the onset and termination for the surface modified sample (inset of Figure 4B) is indicative of faster kinetics, attributed to the presence of ruthenium species on the surface of tin oxide. However, for both the samples the variation of coverage with concentration implies that the kinetics follow the Langmuir adsorption isotherm in the time scale closer to the equilibrium coverage although, deviations can occur due to adsorbate mobility and surface fragmentation. In this range, the curves were fitted with the Langmuir equation to obtain the values of ΔG and adsorption constant (k_a).

The plots from the above data for (a) pure and (b) surface ruthenated tin oxide (600 ppm of butane) and the fitted curves using the Langmuir adsorption isotherm are shown in Figure 5. The Langmuir isotherm[18] dictates that the rate of surface reaction is given by

$$d\theta/dt = k_a(1 - \theta)c + k_d\theta \tag{1}$$

where θ (the coverage of gas on the sensor surface) is the fraction of surface covered, $(1 - \theta)$ is the fraction of the surface exposed, c is the concentration of gas, and k_a and k_d are the adsorption and desorption constants, respectively. Integrating eq 1 gives

$$\theta(t) = (k_ac/k_ac + k_d) [1 - \exp(-k_ac + k_d)t]$$
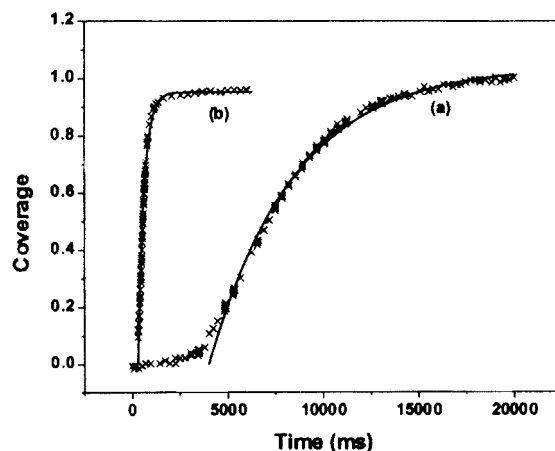
Figure 5. Adsorption kinetics of 600 ppm of LPG on (a) pure and (b) surface ruthenated tin oxide ("×" indicates the actual curves while the solid line indicates the fitted curve).

Substituting $k_ac = k_1$ and $k_ac + k_d = k_2$

$$\theta(t) = k_1/k_2 [1 - \exp(-k_2)t] \tag{2}$$

The raw data was fitted to this curve and it was found that the surface ruthenated sample shows a very good fit while the pure tin oxide shows a fit only between the time scale of 4−20 s (Figure 5). The adsorption kinetics for pure tin oxide in the entire range were tried to fit into the dual site Langmuir isotherm. However, the fit was not good and hence the required parameters were estimated from the Langmuir isotherm fit. The adsorption constants (k_a) obtained from the fitted curves for the pure and ruthenated samples are 8.8 and 1.1×10^2 M^{-1} s^{-1}, respectively, while the desorption constants (k_d) are 1.2×10^{-5} and 1.45×10^{-4} M^{-1} s^{-1}. The higher adsorption and desorption constants of surface ruthenated tin oxide imply that the gas adsorbs and desorbs faster as compared to pure tin oxide. This
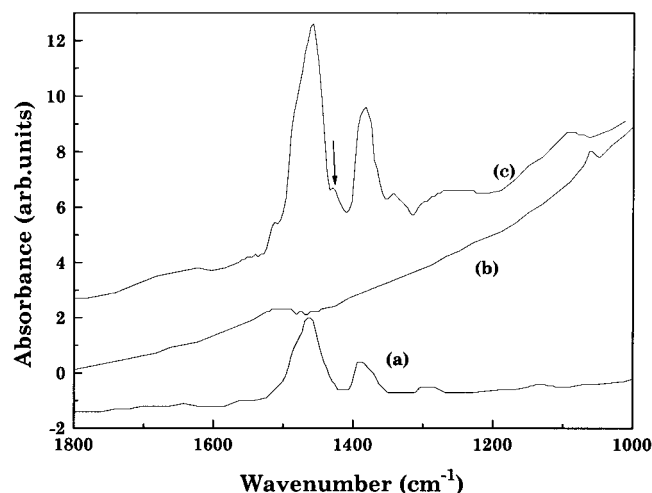
Figure 6. IR spectra of (a) pure butane gas (b) tin oxide exposed to oxygen and (c) tin oxide exposed to butane after conditioning.
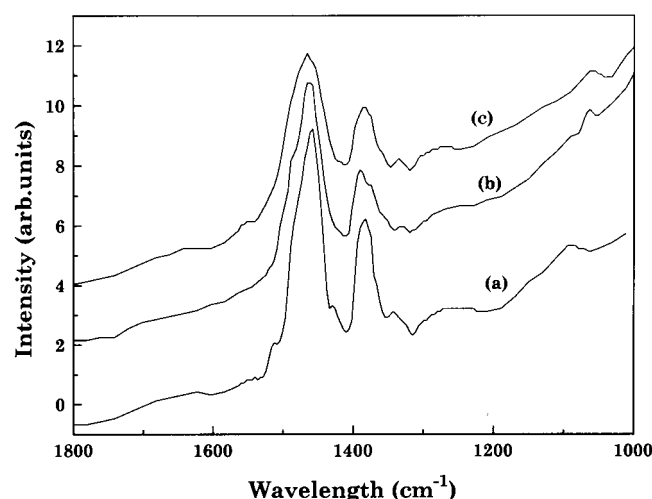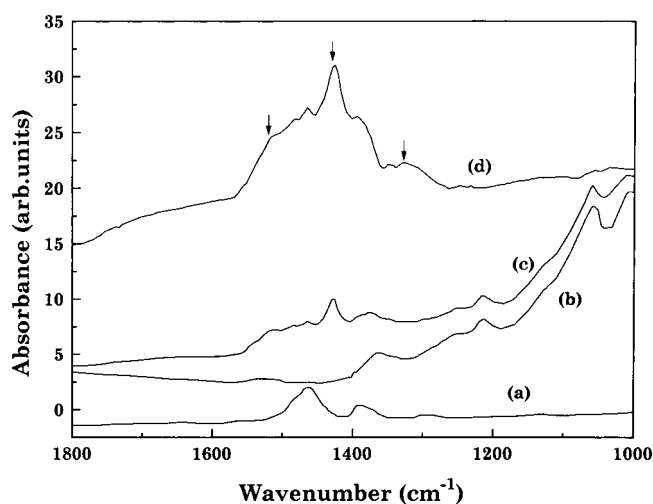

Figure 7. IR spectra of conditioned tin oxide on exposure to butane at (a) 50 °C, (b) 200 °C, and (c) 300 °C.

is in agreement with the fast response and recovery of the ruthenated tin oxide.[15] The adsorption free energy (ΔG) values for the surface ruthenated and tin oxide samples as calculated from the equilibrium constant were found to be -64.85 kJ/mol and -50.2 kJ/mol, respectively.

The IR spectra of pure tin oxide with and without butane gas at 200 °C is shown in Figure 6. The conditioned sample without gas shows a flat spectra except for a small band arising at 1518 cm^{-1} corresponding to the Sn$-$O stretching. On exposure to butane gas adsorption bands arise at 1479, 1465,-1376,1285 and 1140 cm^{-1} with a small shoulder at 1424 cm^{-1}. A comparison with the pure *n*-butane spectrum at the same temperature indicates that the bands at 1479, 1465, 1376, 1285, and 1140 cm^{-1} are due to unreacted butane. The shoulder at 1424 cm^{-1} may be due to some reacted species on the surface of tin oxide. The results indicate that though there may be some reacted species, the conversion may not be very efficient due to less adsorption of gas on the surface (since porosity and hence the surface area is also less).

A comparison of the IR spectra of tin oxide with butane gas at different temperatures shows some interesting differences (Figure 7). The sample at 300 °C shows a very small shoulder at 1424 cm^{-1} which is due to the reacted species on tin oxide. At 200 °C the shoulder is pronounced and more so at 50 °C.

Figure 8. IR spectra of (a) pure butane, and surface ruthenated tin oxide on (b) exposure to oxygen, (c) on exposure to butane after conditioning. [(d) is the subtracted curve which indicates the stretching modes on the surface ruthenated tin oxide at 200 °C].
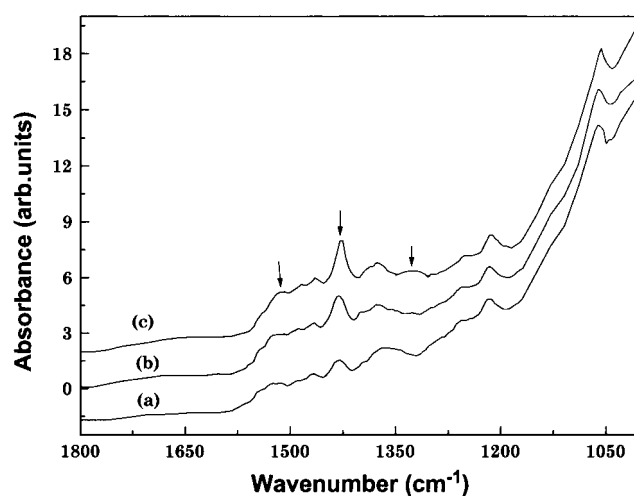

Figure 9. IR spectra of the conditioned surface ruthenated tin oxide on exposure to butane after (a) 10 min, (b) 40 min, and (c) 60 min.
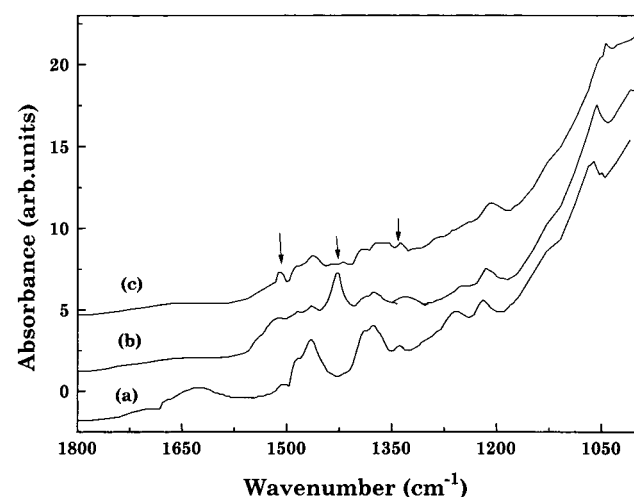
Figure 10. IR spectra of conditioned surface ruthenated tin oxide on exposure to butane at (a) 50 °C, (b) 200 °C, and (c) 300 °C.

The intensity of the absorption band corresponding to the unreacted butane species also increases with decreasing temperature. This implies that, as the temperature decreases more

Surface Ruthenated Tin Oxide

J. Phys. Chem. B, Vol. 105, No. 13, 2001 **2569**

SCHEME 1: Formation of Surface Acetate Species on the Surface Ruthenated Tin Oxide Exposure to Butane at 300 °C and Conversion to Carbon Dioxide and Water
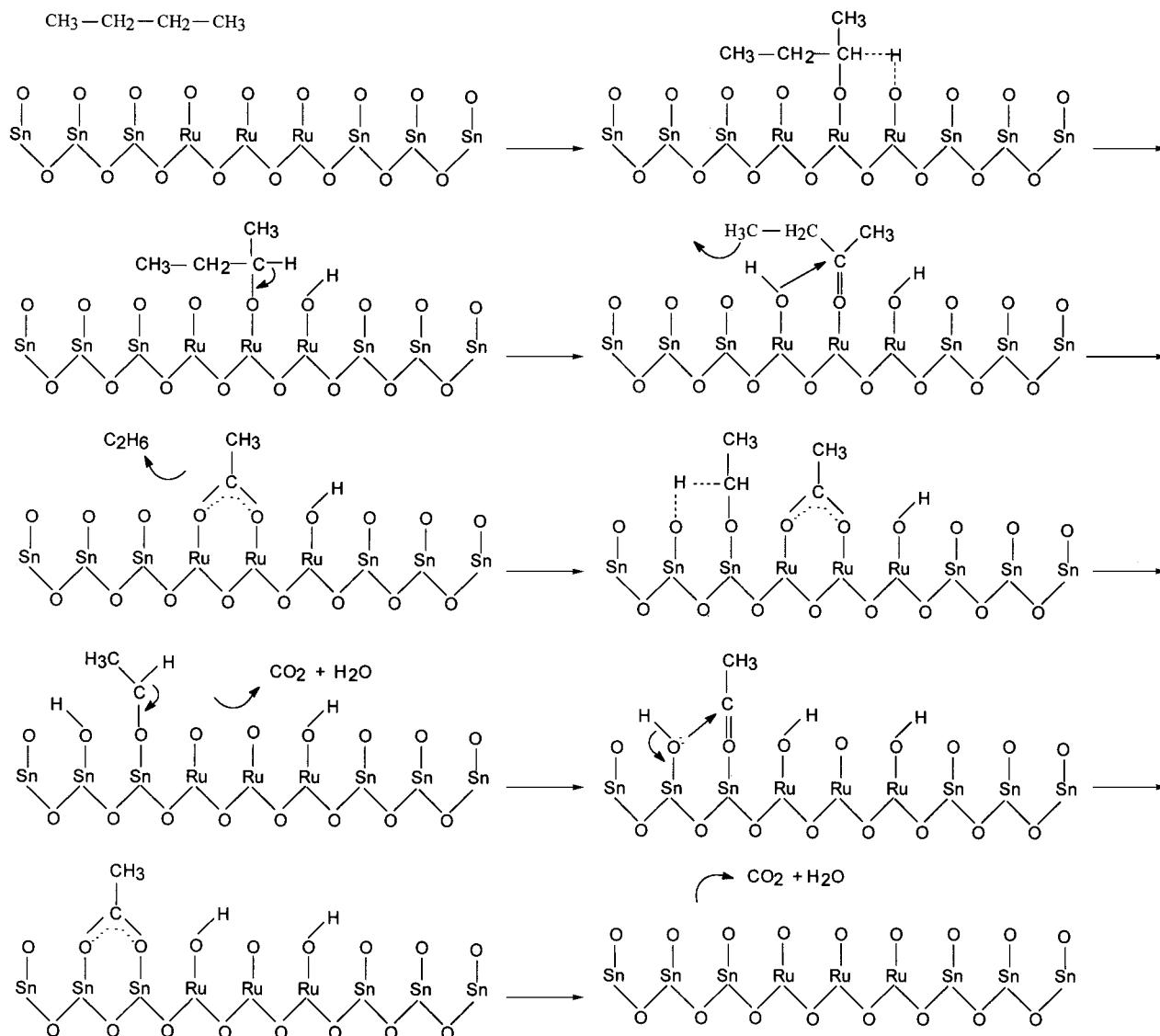

and more unreacted butane may be physisorbed on the sample, which in turn indicates that the catalytic activity of tin oxide is reduced with decreasing temperature. However, the decrease in intensity of the absorption band at 1424 cm^{-1} at 300 °C could be due to complete oxidation of butane through the formation of intermediate species and this species is not detected since it does not adsorb on the sample.

Figure 8 compares the IR spectra of the conditioned surface ruthenated sample with that exposed to butane at 200 °C. The sample without gas shows an absorption band at 1518 cm^{-1} corresponding to Sn−O stretching and the bands at 1354, 1250, and 1211 cm^{-1} corresponding to Ru−O stretching frequency. On exposure to gas absorption bands at 1427 cm^{-1}, 1463 cm^{-1}, 1482, 1512, and 1325 cm^{-1} appear. The observed adsorption bands at 1512, 1427, and 1325 cm^{-1} can be assigned to the antisymmetric and symmetric ν(COO) modes and the symmetric δ (C−H) deformation mode respectively of a surface acetate species.[19] The absorption bands at 1463 and 1482 cm^{-1} correspond to unreacted butane species. These peaks are clearly visible on subtracting the spectra of the conditioned sample from that exposed to butane as shown in the figure.

The IR spectra recorded at different times between 10 min to 1 h after exposure to gas is shown in Figure 9. The sample

exposed to butane gas for 10 min does not show clear adsorption bands at 1512 and 1325 cm^{-1} due to overlapping of the Sn−O stretching at 1518 cm^{-1} and Ru−O stretching at 1359 cm^{-1}. However, with increasing time these bands begin to appear confirming the formation of surface acetate species. The intensity of these bands also increases with time implying that more and more acetate species are being adsorbed on the surface.

The IR spectra of the surface ruthenated tin oxide after exposure to gas were also recorded at different temperatures (Figure 10). The spectrum at 300 °C shows absorption bands at 1512 cm^{-1} and 1325 cm^{-1} while there is a small shoulder corresponding to 1427 cm^{-1}. However, all the bands reduce in intensity as compared to that at 200 °C. It is possible that at higher temperatures butane may undergo complete oxidation forming water and carbon dioxide with surface acetate as the intermediate species. However, at 200 °C the formation of surface acetate is clearly visible. At 50 °C, though a small shoulder is visible at 1512 cm^{-1} and 1325 cm^{-1} corresponding to surface acetate, the bands corresponding to 1463 and 1482 cm^{-1} imply that butane is molecularly adsorbed on the surface. On evacuation of the gas at all three temperatures, the spectra corresponding to bare samples are obtained which indicate that

SCHEME 2: Gas Sensing Mechanism of Surface Ruthenated Tin Oxide Indicating the Role of Surface States in Enhancing the Sensitivity toward Butane
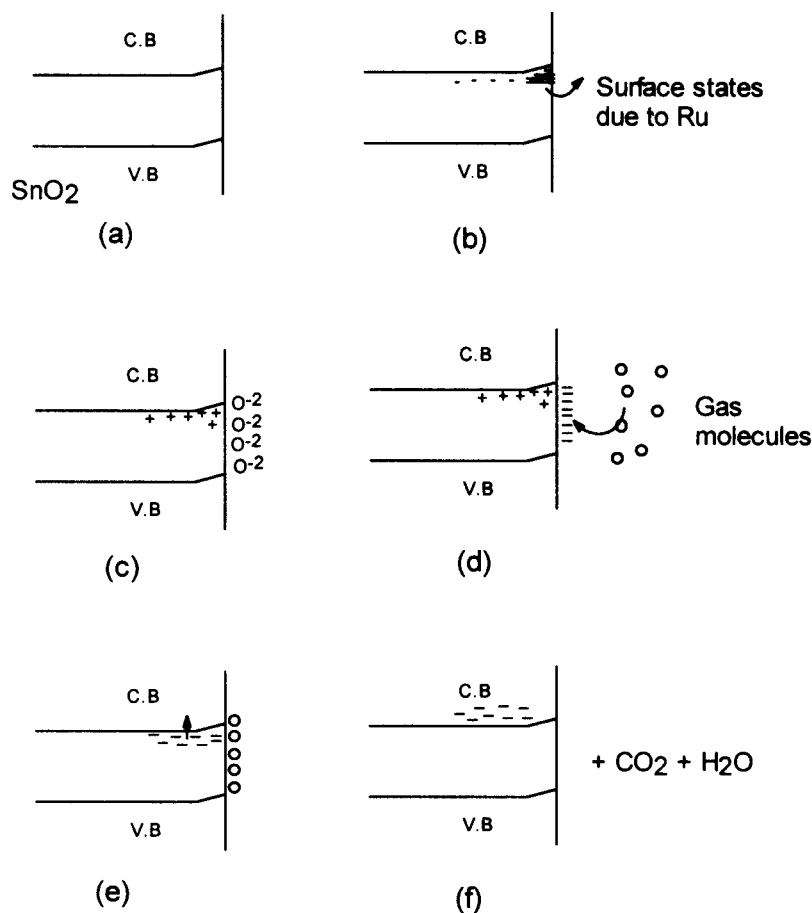
the bonding between the adsorbate and the substrate is very weak.

On the basis of these results we suggest a possible scheme for the gas sensing mechanism for surface ruthenated tin oxide. As the ESR results suggest since Ru sites are more favorable for adsorption, the gas first adsorbs on the Ru sites. Upon adsorption, the butane gas is expected to form a ketonic group via the abstraction of hydrogen groups at two adjacent sites of Ru or Ru and Sn, respectively (Scheme 1). The species then undergoes reaction with the surface hydroxyl groups to produce surface acetate species and ethane. Ethane further adsorbs on the adjacent Ru and Sn sites to form acetate species. At 300 °C the acetate species may form water and carbon dioxide by reacting with oxygen in the atmosphere. Since this reaction is very fast at 300 °C the formation of the intermediate species (acetate groups) is not clearly visible in the IR spectrum.

We have already discussed in our previous work[16] the importance of surface states in enhancing the sensitivity of the surface ruthenated tin oxide. These oxygen species adsorb on the surface of tin oxide abstracting electrons from tin oxide thus causing an increase in the potential barrier. When the gas comes and adsorbs on the surface, by formation of surface acetate there will be electron transfer to the surface states caused by ruthenium near the conduction band edge of tin oxide (Scheme 2) giving rise to Ru^{3+} oxidation state. The energy released during decomposition of the products is sufficient for the electrons to jump into the conduction band of tin oxide thus causing an increase in the conductivity of the sensor element. As the species desorbs from the surface, oxygen is again adsorbed on the tin oxide surface forming O^{2-} or O^- species by abstraction of

electrons from the conduction band causing a decrease in the conductance.

Conclusions

In conclusion, the gas sensing mechanism of surface ruthenated tin oxide involves the adsorption of butane preferentially on the Ru site before undergoing further reaction as implied by the ESR studies. The IR studies imply that the most probable mechanism of butane sensing on the surface ruthenated tin oxide involves the formation of surface acetate species via the abstraction of hydrogen atom by a neighboring oxide species giving a ketonic group formally coordinated to the surface atom. The gas preferentially adsorbs on to the Ru sites causing electron transfer and decreasing the resistance.

References and Notes

(1) Fuller, M. J.; Marwick, M. E. *J. Catal.* **1973**, *29*, 441.
(2) Sermon, P. A.; Self, V. A.; Barret, E. P. S. *J. Mol. Catal.* **1991**, *65*, 395.
(3) Fierro, J. L. G.; Arrua, L. A.; Lopez Neito, J. M.; Kreminic, G. *Appl. Catal* **1998**, *37*, 323.
(4) Briand, D.; Labeau, M.; Gurrie, J. F.; Delabouglise, D. *Sens. Actuators* **1998**, *48*, 395.
(5) Manno, D.; Miccoci, G.; Serra, A.; Tepore, A. *J. Appl. Phys.* **1998**, *83*, 3541.
(6) Shimuzu, Y.; Lin, F. C.; Takao, Y.; Egashira, M. *J. Am. Ceram. Soc* **1998**, *81*, 1633.

Surface Ruthenated Tin Oxide

J. Phys. Chem. B, Vol. 105, No. 13, 2001 **2571**

(7) Ch. Tatsuyama, Sh. Ichimura, Iwakuro, H. *Jpn. J. Appl. Phys.* **1973**, *21*, L25.

(8) Jacquemin, J. L.; Bordure, G. *J. Phys. Chem. Solids* **1974**, *36*, 1081.

(9) Arlinghaus, F. J. *J. Phys. Chem. Solids* **1974**, *35*, 931.

(10) Robertson, J. *J. Phys. C* **1983**, *12*, 4767.

(11) (a) Munnix, S.; Schmeits, M. *Phys. Rev. B* **1983**, *27*, 7624. (b) Munnix, S.; Schmeits, M. *Phys. Rev. B* **1986**, *33*, 4136.

(12) Chaudhary, V. A.; Mulla, I. S.; Vijayamohanan, K. *J. Mater. Res.* **1999**, *14*, 1.

(13) Chaudhary, V. A.; Mulla, I. S.; Vijayamohanan, K. *Sens. Actuators B* **1998**, *50*, 45.

(14) Glassford, K. M.; Chelikowsky, J. R. *Phys. Rev. B* **1993**, *47*, 1732.

(15) Chaudhary, V. A.; Mulla, I. S.; Sainker, S. R.; Belheker, A. A.; Vijayamohanan, K. *Sens. Actutators A* **1998**, *65*, 197.

(16) Chaudhary, V. A.; Mulla, I. S.; Vijayamohanan, K. *Sens. Actuators B* **1999**, *55*, 127.

(17) Shih-Chia Chang, J. *Vac. Sci. Technol.* **1980**, *17*, 336.

(18) Karpovic, D. S.; Blanchard, G. J. *Langmuir* **1994**, *10*, 3315.

(19) Harrison, P. G.; Maunders, B. L. *Chem. Soc. Faraday Trans. 1* **1985**, *81*, 1311.